

Article

Application of Silicon Oxide on High Efficiency Monocrystalline Silicon PERC Solar Cells

Shude Zhang ^{1,2} , Yue Yao ², Dangping Hu ², Weifei Lian ^{2,3}, Hongqiang Qian ², Jiansheng Jie ^{1,*}, Qingzhu Wei ^{2,4,*}, Zhichun Ni ^{2,3}, Xiaohong Zhang ¹ and Lingzhi Xie ⁵

¹ Jiangsu Key Laboratory for Carbon-Based Functional Materials & Devices, Institute of Functional Nano & Soft Materials (FUNSOM), Soochow University, Suzhou 215123, China; shude.zhang@talesun.com (S.Z.); xiaohong_zhang@suda.edu.cn (X.Z.)

² Suzhou Talesun Solar Technologies Co., Ltd., Changshu 215542, China; yue.yao@talesun.com (Y.Y.); dangping.hu@talesun.com (D.H.); weifei.lian@talesun.com (W.L.); hongqiang.qian@talesun.com (H.Q.); paul@talesun.com (Z.N.)

³ Nanjing University of Aeronautics & Astronautics, Nanjing 210016, China

⁴ Changshu Institute of Technology, Changshu 215500, China

⁵ Institute of New Energy and Low-carbon Technology, Sichuan University, Chengdu 610065, China; xielingzhi@scu.edu.cn

* Correspondence: jsjie@suda.edu.cn (J.J.); qingzhu.wei@talesun.com (Q.W.)

Received: 31 December 2018; Accepted: 21 March 2019; Published: 26 March 2019



Abstract: In the photovoltaic industry, an antireflection coating consisting of three SiN_x layers with different refractive indexes is generally adopted to reduce the reflectance and raise the efficiency of monocrystalline silicon PERC (passivated emitter and rear cell) solar cells. However, for SiN_x , a refractive index as low as about 1.40 cannot be achieved, which is the optimal value for the third layer of a triple-layer antireflection coating. Therefore, in this report the third layer is replaced by SiO_x , which possesses a more appropriate refractive index of 1.46, it and can be easily integrated into the SiN_x deposition process with the plasma-enhanced chemical vapor deposition (PECVD) method. Through simulation and analysis with SunSolve, three different thicknesses were selected to construct the SiO_x third layer. The replacement of 15 nm SiN_x with 30 nm SiO_x as the third layer of antireflection coating can bring about an efficiency gain of 0.15%, which originates from the reflectance reduction and spectral response enhancement below about 550 nm wavelength. However, because the EVA encapsulation material of the solar module absorbs light in short wavelengths, the spectral response advantage of solar cells with 30 nm SiO_x is partially covered up, resulting in a slightly lower cell-to-module (CTM) ratio and an output power gain of only 0.9 W for solar module.

Keywords: silicon oxide; silicon nitride; triple-layer antireflection coating; monocrystalline silicon PERC solar cell

1. Introduction

Antireflection coating plays an important role in the improvement of short-circuit current density and photovoltaic conversion efficiency of silicon solar cells. With antireflection coating, the reflectance can be greatly decreased across the whole absorption band [1]. To achieve minimum reflection of a normal incident wave of a single wavelength, the antireflection coating may consist of a single layer, which must possess (a) a refractive index equal to the square root of the refractive indices of the materials bounding the coating and (b) a thickness equal to one-quarter of the wavelength within the material of which the coating consists [1], as shown in Equations (1) and (2). When the design wavelength is 550 nm (λ_{air}), the optimal refractive index and thickness of the single-layer antireflection

coating are determined as 1.85 and 74 nm ($n_{air} = 1.00$, $n_{Si} = 3.42$). Up to now, several materials have been adopted for a single-layer antireflection coating, such as TiO_2 , SiO_2 , and so on [2,3].

$$n = \sqrt{n_{air} n_{Si}}, \quad (1)$$

$$d = \frac{\lambda_{air}}{4n}. \quad (2)$$

However, if one wants to achieve broadband antireflection coatings, additional layers must be added [1]. For a double-layer antireflection coating, the design can be optimized with Equations (3) and (4) according to the report of Richards [4]. The refractive indexes are stacked as follows $n_{Si} > n_{1st} > n_{2nd} > n_{air}$, where n_{1st} and n_{2nd} represent the refractive indexes of the first layer and second layer of the antireflection coating. When the design wavelength is 550 nm (λ_{air}), the optimal refractive indexes and thicknesses of each layer are determined as 2.27 (n_{1st}), 1.51 (n_{2nd}), 61 nm (d_{1st}), and 91 nm (d_{2nd}). In consideration of the practical materials, Al_2O_3 was combined with TiO_2 [5], and MgF_2 was combined with ZnS [6] to construct the double-layer antireflection coating.

$$n_{1st}^3 = n_{air} n_{Si}^2, n_{2nd}^3 = n_{air}^2 n_{Si}, \quad (3)$$

$$d_{1st} = \frac{\lambda_{air}}{4n_{1st}}, d_{2nd} = \frac{\lambda_{air}}{4n_{2nd}}. \quad (4)$$

According to the report of Bouhafs et al. [7], the design of a triple-layer antireflection coating on silicon can be optimized with Equations (5)–(7), where n_{1st} , n_{2nd} , and n_{3rd} are the refractive indexes of first layer, second layer, and third layer, respectively. The refractive index decreases in the order $n_{Si} > n_{1st} > n_{2nd} > n_{3rd} > n_{air}$. When the design wavelength is 550 nm (λ_{air}), the optimal refractive indexes and thicknesses of each layer are determined as 2.52 (n_{1st}), 1.85 (n_{2nd}), 1.36 (n_{3rd}), 55 nm (d_{1st}), 74 nm (d_{2nd}), and 101 nm (d_{3rd}). Triple-layer antireflection coatings, e.g., $SiO_2/SiO_2-TiO_2/TiO_2$ [1] and $SiO_x/SiO_xN_y/SiN_x$ [8], were adopted to decrease the reflectance and increase the efficiency of silicon solar cells.

$$n_{2nd}^2 = n_{1st} n_{3rd} = n_{air} n_{Si}, \quad (5)$$

$$n_{1st}^2 = n_{Si} n_{2nd}, n_{3rd}^2 = n_{2nd} n_{air} \quad (6)$$

$$d_{1st} = \frac{\lambda_{air}}{4n_{1st}}, d_{2nd} = \frac{\lambda_{air}}{4n_{2nd}}, d_{3rd} = \frac{\lambda_{air}}{4n_{3rd}}. \quad (7)$$

Apparently, the triple-layer antireflection coating shows the lowest reflectance in these three structures [1]. Therefore, the photovoltaic industry is very willing to adopt the triple-layer structure for a better photovoltaic performance. In spite of the appropriate refractive index ($n = 2.26$) as the first layer of a triple-layer antireflection coating, TiO_2 seems not to be the best choice on account of its poor surface passivation capability, which is unbeneficial to the open circuit voltage of a solar cell [1]. As for SiN_x , on the one hand, its refractive index can be easily tuned from 1.98 to 2.98 in the deposition process with the PECVD (plasma-enhanced chemical vapor deposition) method [9]. On the other hand, resulting from the high density of fixed positive charges and high hydrogen content, SiN_x possesses outstanding surface passivation ability, which is beneficial for the improvement of an open circuit voltage [8]. Therefore, in the photovoltaic industry, the antireflection coating is generally made up of three SiN_x layers with different refractive indexes deposited by PECVD, in consideration of the antireflection effect, surface passivation, and simplicity of the process.

Although the surface passivation effect of SiN_x can be improved along with the increase of refractive index, the parasitic absorption becomes more severe. Therefore, for balance, the refractive index of the first SiN_x layer is usually around 2.37 (n_{1st}). Correspondingly, the optimal refractive indexes of the other two SiN_x layers are determined as 1.85 (n_{2nd}) and 1.44 (n_{3rd}) according to Equation (5). When the design wavelength is 550 nm (λ_{air}), the optimal thicknesses of each SiN_x layer are determined as 58 nm (d_{1st}), 74 nm (d_{2nd}), and 95 nm (d_{3rd}), according to Equation (7).

However, it can be found that the refractive indexes of the second and third layers cannot be achieved by SiN_x [9]. Therefore, Kuo et al. adopted SiO_xN_y ($n = 1.8$) as the second layer and SiO_x ($n = 1.46$) as the third layer [8], both of which can be easily integrated into the SiN_x deposition process with the PECVD method. In actual production of crystalline silicon solar cells, 240 pieces are deposited with antireflection coating in a PECVD tube furnace simultaneously, which means that the control of consistency between each piece is of particular importance. When SiO_xN_y is being deposited, three gases (SiH_4 , NH_3 , and N_2O) need to be injected into the tube furnace at the same time, which is a big challenge for the control of consistency. Kuo et al. used the calculated optimal thicknesses (59.78, 76.39, and 94.18 nm) as the actual thicknesses of each layer, which resulted in an impressive antireflection effect [8]. However, the entire thickness was up to 230 nm, which significantly increases the cost of the antireflection coating. In addition, on account of the fire-through silver contact metallization applied, a coating thickness up to 230 nm definitely influences the contact between silver and silicon. Therefore, to balance the cost, electrode contact, and antireflection effect, the entire thickness of the antireflection coating is usually around 80 nm in mass production.

Hence, in this report, in order to seek a more feasible antireflection coating structure with lower reflectance in mass production, SiO_x was adopted to replace the third layer of traditional, triple-layer SiN_x antireflection coating, preserving the other two layers. This new kind of antireflection coating was applied to improve the efficiency of a monocrystalline silicon PERC (passivated emitter and rear cell) solar cell, which is anticipated to dominate the photovoltaic market in the next few years.

2. Materials and Methods

Boron-doped monocrystalline silicon wafers with a length of 156.75 mm, thickness of 180 μm , and resistivity of about $0.8 \Omega\cdot\text{cm}$ were adopted. The manufacturing process flow of an industrialized monocrystalline silicon PERC solar cell is shown in Figure 1.

The as-cut monocrystalline silicon wafers were firstly textured with an alkali-based etching solution. Then, the samples were transferred into a tubular furnace to complete phosphorous diffusion and emitter formation. Subsequently, phosphosilicate glass (PSG) removal, edge isolation, and rear surface polishing were accomplished with a wet etching technique. After that, the aluminum oxide and silicon nitride were deposited by ALD (atomic layer deposition) and PECVD successively to form the passivation stack ($\text{Al}_2\text{O}_3/\text{SiN}_x$) on the rear surface. Afterwards, the PECVD was still used to deposit the antireflection coating on the front surface. After the $\text{Al}_2\text{O}_3/\text{SiN}_x$ stack was locally opened by laser ablation, the electrode pastes (rear-side silver, rear-side aluminum, and front-side silver) were screen-printed and dried. Finally, the samples were sintered in a mesh belt furnace to complete the metallization and finish the solar cell manufacturing process.

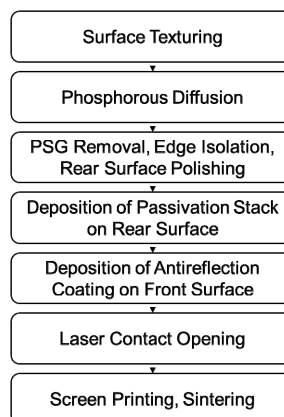


Figure 1. The manufacturing process flow of industrialized monocrystalline silicon solar cells.

During the deposition of the antireflection coating, the gas sources were changed to adjust the layer composition. For SiN_x , silicane (SiH_4) and ammonia (NH_3) were adopted as the gas sources.

And for SiO_x , the ammonia was replaced by laughing gas (N_2O). In detail, two SiN_x layers with different refractive indexes ($n = 2.37$ and $n = 2.09$) and one SiO_x layer ($n = 1.46$) were combined to form the triple-layer antireflection coating. As mentioned above, the control of consistency is particularly important because 240 samples are simultaneously fabricated in a tube furnace. The gas flows (SiH_4 and N_2O), pressure, radio-frequency power, and temperatures of different zones were adjusted and optimized in order to improve the consistency. The results shown below were obtained after the optimization. For comparison, the traditional SiN_x triple-layer antireflection coating was also adopted to manufacture solar cells, i.e., employing the SiN_x layer with a refractive index of 1.99 as the third layer.

After the completion of the whole manufacturing process flow of the solar cell, the passivation of carrier-induced defects was conducted by current injection to suppress the severe light-induced degradation of the PERC solar cell.

Before the experiment, a theoretical analysis was conducted to explore the optimal thickness of the SiO_x layer. As for textured wafers, the light travels through the antireflection coating obliquely, which will increase the optical path length. Additionally, the fraction of light initially reflected from the surface can hit the surface a second time and has another opportunity to enter the wafer [10]. Therefore, in view of these differences with planar wafers, a simulation software called SunSolve from PV Lighthouse was adopted, instead of the equations mentioned above, to further improve the accuracy of the theoretical analysis. Combining Monte Carlo ray-tracing with thin-film optics, SunSolve can determine the optical losses in a solar cell or solar module under a chosen spectrum [11].

As shown in Figure 2, the simulation structure consisted of a triple-layer antireflection coating, a random upright pyramid texture with a height of 2 μm , a monocrystalline silicon wafer with a thickness of 170 μm , a planar rear surface, an $\text{Al}_2\text{O}_3/\text{SiN}_x$ passivation stack, and an aluminum electrode from top to bottom. The front busbars and fingers were excluded to focus on the antireflection coating.

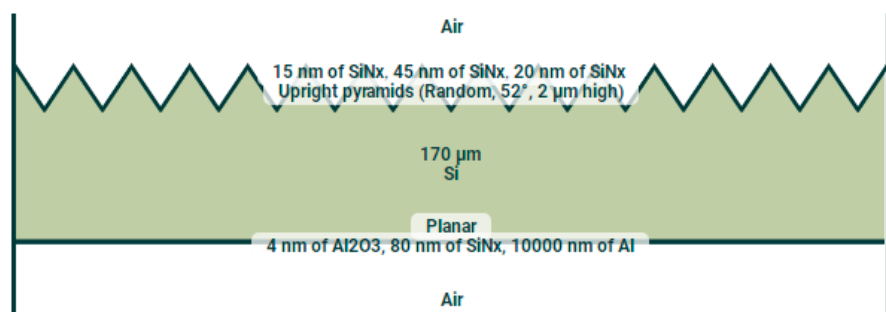


Figure 2. The simulation structure of monocrystalline silicon PERC solar cells in SunSolve. The front busbars and fingers are excluded to focus on the antireflection coating.

The simulation parameters of the triple-layer antireflection coating are listed in Table 1. The parameters of the first SiN_x layer and second SiN_x layer were fixed as 20 nm ($n = 2.37$) and 45 nm ($n = 2.09$), respectively. The parameters of the third layer were adjusted, including material, refractive index, and thickness.

Table 1. The simulation parameters of the triple-layer antireflection coating of monocrystalline silicon PERC solar cells in SunSolve.

| Code Name | First SiN_x Layer $n = 2.37$ | Second SiN_x Layer $n = 2.09$ | Third Layer |
|-----------|---------------------------------------|--|-------------------------------------|
| A | 20 nm | 45 nm | 15 nm SiN_x ($n = 1.99$) |
| B1 | 20 nm | 45 nm | 10 nm SiO_x ($n = 1.46$) |
| B2 | 20 nm | 45 nm | 20 nm SiO_x ($n = 1.46$) |
| B3 | 20 nm | 45 nm | 30 nm SiO_x ($n = 1.46$) |
| B4 | 20 nm | 45 nm | 40 nm SiO_x ($n = 1.46$) |
| B5 | 20 nm | 45 nm | 50 nm SiO_x ($n = 1.46$) |

3. Results

3.1. Simulation Results

The simulated reflectance curves of the monocrystalline silicon PERC solar cell with different third layers of antireflection coating in SunSolve are shown in Figure 3. It can be found that below about 550 nm, samples with SiO_x as the third layer possessed a much lower reflectance than samples with SiN_x as the third layer. Along with the increase in thickness of the SiO_x third layer, the reflectance below about 400 nm decreased. On the contrary, between 400 nm and 550 nm, the reflectance increased. It was interesting that above about 600 nm, the reflectance decreased as well in the wake of an increasing thickness. When the SiO_x thickness fell in between 30 nm and 40 nm, the reflectance of the SiO_x third layer sample was close to the SiN_x third layer sample above about 600 nm.

According to the report of Bouhafs et al. [7], the weighted average reflectance (WAR) was calculated using the following Equation (8), because the solar cell performance was also influenced by the photon flux and internal quantum efficiency. $F_i(\lambda)$, $Q_i(\lambda)$, and $R(\lambda)$ represent the photon flux, internal quantum efficiency, and reflectance, respectively, at the wavelength λ_i (λ_1 (300 nm) $\leq \lambda_i \leq \lambda_2$ (1100 nm)). The internal quantum efficiency data came from a monocrystalline silicon PERC solar cell. The corresponding WAR values of each antireflection coating are listed in Figure 3.

$$\text{WAR} = \frac{\int_{\lambda_1}^{\lambda_2} F_i(\lambda) Q_i(\lambda) R(\lambda) d\lambda}{\int_{\lambda_1}^{\lambda_2} F_i(\lambda) Q_i(\lambda) d\lambda}. \quad (8)$$

It can be found that along with the increase in the thickness of the SiO_x third layer, the WAR decreased from 3.13% (10 nm SiO_x) to 2.46% (50 nm SiO_x). Apparently, the substitute of 15 nm SiN_x with 10 nm SiO_x as the third layer cannot improve the reflectance, which meant that the SiO_x thickness should be at least 20 nm. On the other hand, in consideration of the fire-through silver contact metallization applied, the increase in thickness of the triple-layer antireflection coating was limited to guarantee efficient contact between silver and silicon. Therefore, three SiO_x thicknesses were employed in the following experiments, at 20 nm, 30 nm, and 40 nm.

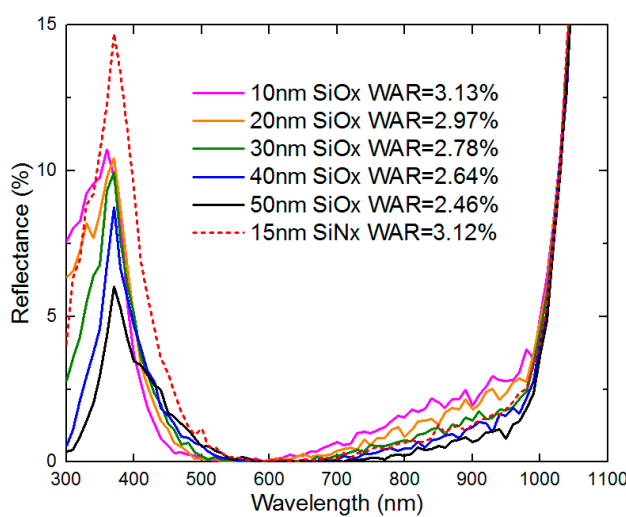


Figure 3. The simulated reflectance curves of monocrystalline silicon PERC solar cells with different third layers of antireflection coating in SunSolve. The corresponding weighted average reflectances (WARs) are listed.

3.2. Solar Cell

According to the simulation results, SiO_x third layers with three different thicknesses were employed to construct the antireflection coating, i.e., 20 nm, 30 nm, and 40 nm, resulting in three

groups of monocrystalline silicon PERC solar cells. A group with a 15 nm SiN_x third layer served as a control. Each group contained about 100 samples, and the photovoltaic parameters are exhibited in box plots (Figure 4). It can be found that because of the presence of a few outliers, some mean values were significantly lower than the median values. Therefore, the median values were extracted and listed in Table 2, which could better reflect the practical situation. In addition, the efficiency gains compared with the 15 nm SiN_x group in Figure 4d were calculated with median values as well. It showed that the replacement of SiN_x with SiO_x as the third layer could effectively improve the short-circuit current (I_{sc}). When the 20 nm SiO_x third layer could bring about a current gain of 40 mA, another gain above 20 mA could be achieved by increasing the SiO_x thickness to 30 nm or 40 nm. This current improvement was in accordance with the simulation results, which showed that the reflectance declined in short wavelengths. Except for the current, the other two photovoltaic parameters, i.e., open circuit voltage (V_{oc}) and fill factor (FF), had little variation, which implied that the replacement of SiN_x with SiO_x as the third layer made no difference in the front surface passivation and front grid metallization. As a result, the photovoltaic conversion efficiency (Eff) was improved, owing to the improvement of short-circuit current. Because of the very similar currents, the 30 nm and 40 nm SiO_x groups had very similar efficiencies, which were about 0.15% (abs.) higher than the SiN_x group. In addition, from the box plots shown in Figure 4, it can be found that this replacement of SiN_x with SiO_x as the third layer had a negative impact on the current distribution to a certain extent, which resulted in a slight widening of the efficiency distribution. As mentioned above, the PECVD device adopted was designed for industrial production, and 240 samples were simultaneously fabricated in a tube furnace. Although we adjusted and optimized the deposition conditions to improve the consistency, such as gas flows (SiH_4 and N_2O), pressure, radio-frequency power, and temperatures of different zones, the conditions still needed to be fine-tuned to further reduce the distribution width and the number of outliers.

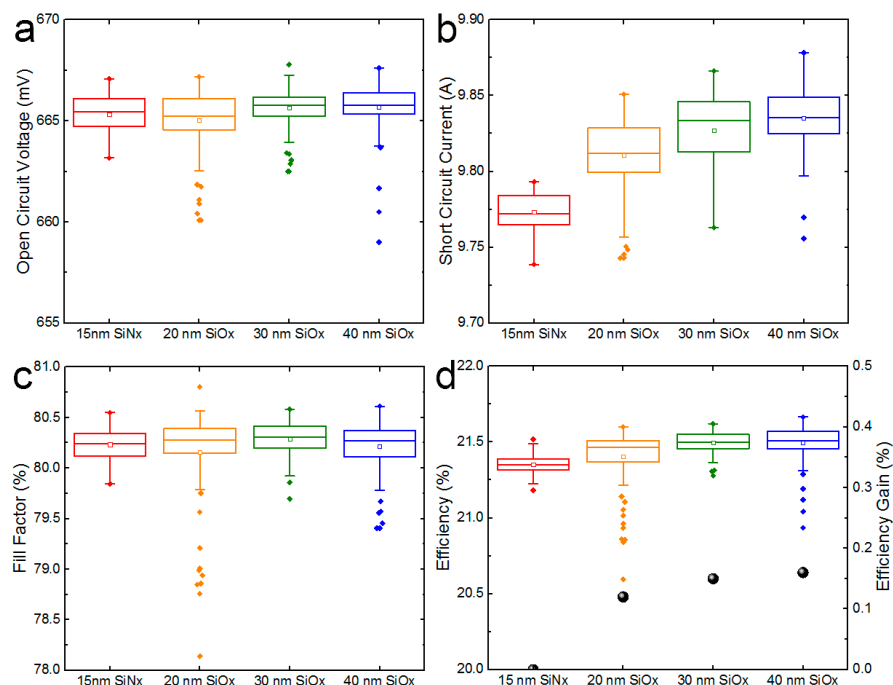


Figure 4. Box plots of the photovoltaic parameters (a—open circuit voltage, b—short-circuit current, c—fill factor, and d—efficiency) of the monocrystalline silicon PERC solar cells fabricated with different third layers of antireflection coating. Each group contained about 100 solar cells. The outliers and mean values are represented by solid lozenges and hollow squares. The solid black spheres in d represent the median efficiency gains compared with the 15 nm SiN_x group.

Table 2. The photovoltaic parameters of the monocrystalline silicon PERC solar cells fabricated with different third layers of antireflection coating. Each group contained about 100 solar cells, and the median values are listed.

| Group | V_{OC} (mV) | I_{SC} (A) | FF (%) | Eff (%) |
|------------------------|---------------|--------------|--------|---------|
| 15 nm SiN _x | 665.5 | 9.772 | 80.25 | 21.35 |
| 20 nm SiO _x | 665.2 | 9.812 | 80.28 | 21.47 |
| 30 nm SiO _x | 665.8 | 9.834 | 80.31 | 21.50 |
| 40 nm SiO _x | 665.8 | 9.836 | 80.27 | 21.51 |

In order to investigate the origin of current improvement, the reflectance and external quantum efficiency (EQE) were measured. It should be noted that because industrial production equipment was adopted to deposit the antireflection coating, the group differences between thicknesses where SiO_x was the third layer might be covered up by the normal fluctuation. Therefore, only one group of the SiO_x third layers was chosen to compare with the SiN_x group. In consideration of the efficiency gain and economy, a 30 nm SiO_x third layer was the optimal choice because it had a very similar efficiency gains and consumed less raw materials, compared with the 40 nm SiO_x one. The reflectance curves of one 30 nm SiO_x sample and one 15 nm SiN_x sample before metallization are shown in Figure 5a, and the EQE curves after metallization are exhibited in Figure 5b. Because of the limitation of corresponding test instruments, there was a slight difference between two wavelength ranges in Figure 5, i.e., 350–1050 nm for reflectance and 300–1100 nm for EQE. The reflectance curves were smoothed to make the results easier to observe. It can be found that compared with the 15 nm SiN_x sample, the 30 nm SiO_x sample possessed a significantly lower reflectance below about 550 nm and almost the same reflectance above about 600 nm, which was in accordance with the simulation results. After metallization, the 30 nm SiO_x sample possessed a significantly higher EQE below about 550 nm and almost the same EQE above about 600 nm, which complied well with the reflectance results. On account of the EQE improvement, the 30 nm SiO_x sample exhibited a higher short-circuit current, which verified the above photovoltaic parameters.

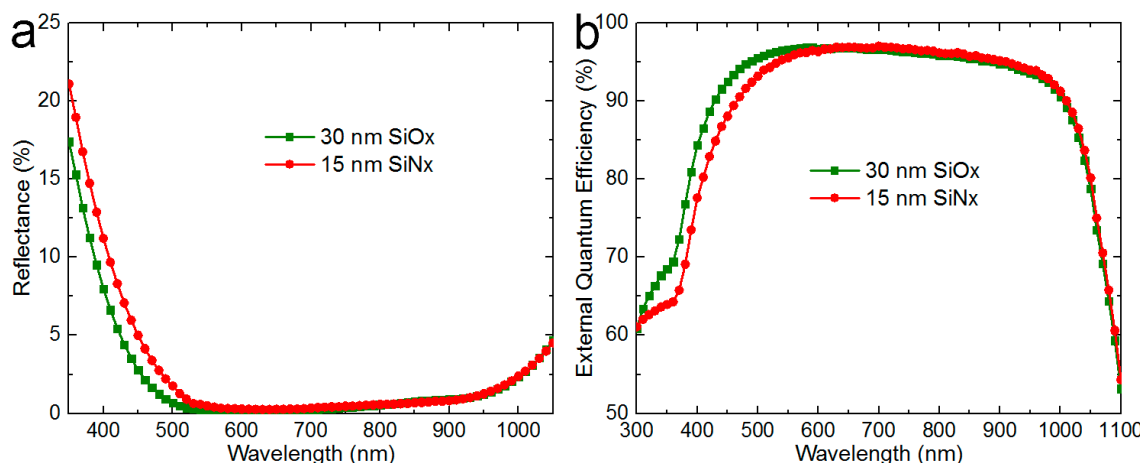


Figure 5. (a) Reflectance curves of the 30 nm SiO_x third layer sample and the 15 nm SiN_x third layer sample before metallization. (b) External quantum efficiency curves of the 30 nm SiO_x third layer sample and the 15 nm SiN_x third layer sample after metallization.

3.3. Solar Module

In order to examine whether the monocrystalline silicon PERC solar cells based on SiO_x as the third layer of antireflection coating had reliability problems, solar modules needed to be fabricated. As mentioned above, the thickness of 30 nm was considered to be the optimal choice for SiO_x as the third layer of antireflection coating. Therefore, another 1200 monocrystalline silicon PERC solar cells

with 30 nm SiO_x were fabricated, and the whole 1300 solar cells were sorted according to the efficiency. Consequently, 480 solar cells with the efficiency level of 21.5% ($21.5\% \leq \text{Eff} < 21.6\%$) were picked out to fabricate eight solar modules. Two solar modules were used to examine the light-induced degradation (LID), and another two ones were used to examine the potential-induced degradation (PID). Standard test conditions were adopted, i.e., LID: 1000 W/m², 60 °C, and 60 h; PID: 85 °C, 85% RH (relative humidity), -1000 V, and 192 h for PID. Solar modules with 15 nm SiN_x served as a control. The mean cell-to-module (CTM) ratios, LID rates, and PID rates of monocrystalline silicon PERC solar modules with different third layers of antireflection coating, i.e., 30 nm SiO_x and 15 nm SiN_x , are listed in Table 3. It was apparent that the solar modules with 30 nm SiO_x possessed a slightly lower CTM ratio than those with 15 nm SiN_x , which could be ascribed to the spectral response advantage below about 550 nm. It is known that the EVA (ethylene vinyl acetate copolymer) encapsulation material of the solar module will absorb light in short wavelengths, resulting in the partial cover-up of corresponding spectral response advantages. According to the CTM ratios, it could be deduced that the replacement of 15 nm SiN_x with 30 nm SiO_x could bring about an average output power gain of 0.9 W for the solar module. The LID and PID rates of 30 nm SiO_x solar modules were close to those of 15 nm SiN_x . Besides, from the electroluminescence images before and after the LID test (Figure 6b) or PID test (Figure 6c,d), there were no severely degraded solar cells existing in the solar modules, which verified the consistency of solar cells with 30 nm SiO_x as the third layer of antireflection coating. Therefore, this new kind of antireflection coating will not negatively affect the reliability of the solar module.

Table 3. Cell-to-module ratios, light-induced degradation (LID) rates, and potential-induced degradation (PID) rates of monocrystalline silicon PERC solar modules with different third layers of antireflection coating, i.e., 30 nm SiO_x and 15 nm SiN_x . Mean values and the CTM standard deviation values are listed. The LID test conditions are 1000 W/m², 60 °C, and 60 h. The PID test conditions are 85 °C, 85% RH (relative humidity), -1000 V, and 192 h.

| Group | CTM (%) | LID (%) | PID (%) |
|----------------------|-------------|---------|---------|
| 30 nm SiO_x | 96.1 (0.30) | 2.3 | 2.7 |
| 15 nm SiN_x | 96.5 (0.33) | 2.4 | 2.5 |

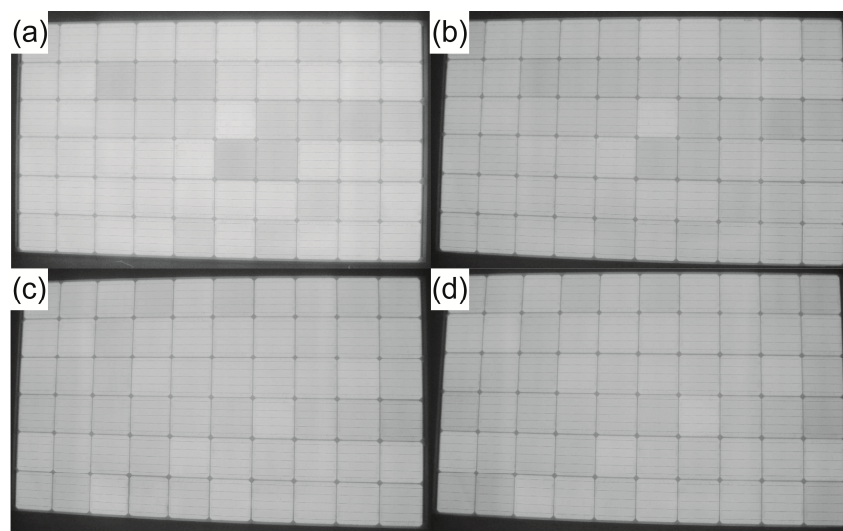


Figure 6. Electroluminescence images of monocrystalline silicon PERC solar modules with 30 nm SiO_x as the third layer of antireflection coating before and after the LID test (a,b) or PID test (c,d).

4. Further Discussion

In the results above, there is a lack of internal quantum efficiency data, which are essential in assessing the parasitic absorption of antireflection coating. Therefore, in order to solve this

problem, new solar cell samples with different third layers (i.e. 15 nm SiN_x and 30 nm SiO_x) of antireflection coating have been fabricated recently. Each group contained about 400 solar cells, and the mean photovoltaic parameters are listed in Figure 7. It should be noted that because several other optimization methods have been applied, such as wafer resistivity reduction, phosphorus-doping profile adjustment, and surface passivation improvement with a thermally grown SiO₂ thin layer (~2 nm), photovoltaic performance has made good progress. On this basis, the alteration of the third layer of antireflection coating leads to a short-circuit current gain of 56 mA and an efficiency gain of 0.13% (abs.), when the open circuit voltage and fill factor remain almost unchanged. The reflectance, external quantum efficiency, and internal quantum efficiency of two kinds of solar cells were measured, as shown in Figure 7. It can be found that the reflectance and EQE improved in short wavelengths after the alteration, which was consistent with the previous results. On the contrary, the IQE suffered a decline below about 400 nm. On the one hand, the altered layer of antireflection coating was the third layer, which was not in direct contact with the silicon substrate. On the other hand, the open circuit voltage barely changed according to both previous and current results. Therefore, it is believed that the surface passivation will not be influenced by the alteration of the third layer of antireflection coating. Correspondingly, the IQE decline below about 400 nm could be ascribed to the increase in parasitic absorption, which may be induced by SiO_x.

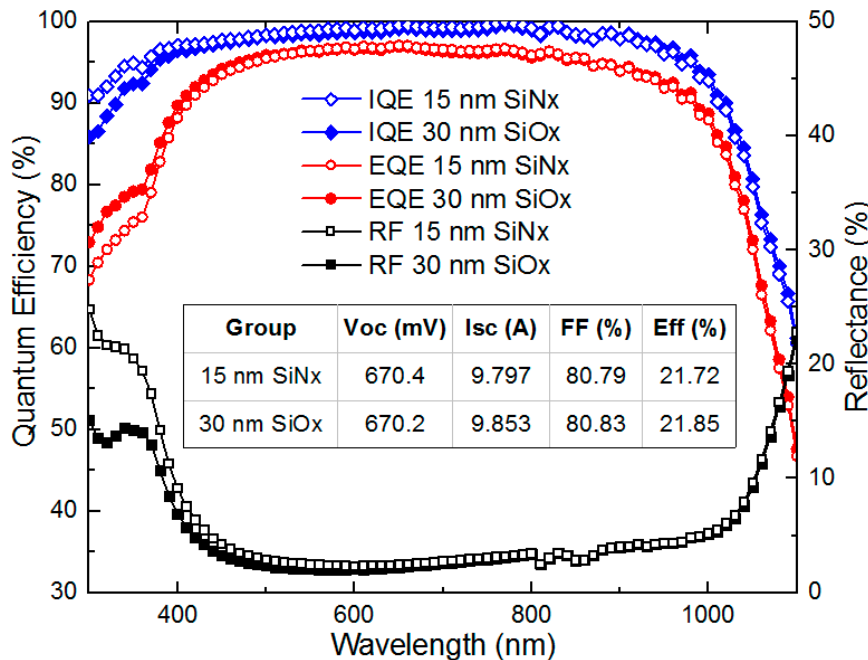


Figure 7. Reflectance (RF), external quantum efficiency (EQE), and internal quantum efficiency (IQE) curves of monocrystalline silicon PERC solar cells with the 15 nm SiN_x third layer and the 30 nm SiO_x third layer as the antireflection coating. The mean photovoltaic parameters of each group containing about 400 solar cells are listed.

As a matter of fact, except the optimization for air in this report, the antireflection coating of the solar cell can be optimized directly for the glass/EVA encapsulation, which is expected to be more beneficial for the improvement of the solar module's output power. However, this strategy is somewhat infeasible, because almost all of the characterization methods for solar cells are conducted in air, such as IV (current-voltage), QE (quantum efficiency), and reflectance. Nevertheless, the differences between these two strategies can be discussed according to theoretical calculations and experimental results. As mentioned above, the refractive index of the first SiN_x layer of antireflection coating is usually around 2.37. According to Equation (5) (n_{air} is replaced by n_{EVA}), the optimal refractive indexes of the other two SiN_x layers are determined as 2.26 (n_{2nd}) and 2.15 (n_{3rd}) for the glass/EVA encapsulation

($n_{\text{glass}} = n_{\text{EVA}} = 1.50$). In contrast, the values are 1.85 ($n_{2\text{nd}}$) and 1.44 ($n_{3\text{rd}}$) for air, which are much lower than those for encapsulation. From another viewpoint, the gain/loss induced by the different optical environments can be estimated according to the experimental results. When the SiN_x third layer of antireflection coating is replaced by SiO_x , the relative performance improvements of the solar cell and the solar module are 0.70% (absolute 0.15%) and 0.30% (absolute 0.9 W), respectively. It can be deduced that the performance gain in solar cells is reduced by 57% when implementing the SiO_x in the modules.

5. Prospects

In this report, a triple-layer structure was adopted to construct the antireflection coating of monocrystalline silicon PERC solar cells. However, only the third layer of antireflection coating was adjusted and optimized, the other two layers were fixed. This structure modification brought about an efficiency gain of 0.15% for the solar cell. It can be expected that if the other two layers also take part in the optimization of antireflection coating, the reflectance and conversion efficiency of the solar cell will be further improved.

On the other hand, except for further improvement in the solar cell, attention should also be paid to the solar module. The absorption of EVA encapsulation material in short wavelengths results in the partial cover-up of the spectral response advantage of the solar cell with SiO_x as the third layer, which leads to an output power gain of only 0.9 W for solar module. Therefore, through enhancing the encapsulation material transmittance in short wavelengths, the CTM ratio can be increased, and a higher output power gain is expected to be achieved.

At present, further optimization of antireflection coating is in progress, and an average efficiency gain of 0.2% for solar cells has been achieved. Combined with wafer resistivity reduction, phosphorus-doping profile adjustment, and surface passivation improvement, the average efficiency of monocrystalline silicon PERC solar cells grows to 21.93%. It should be noted that if selective emitter technology is applied, the solar cell efficiency is expected to reach 22.1%. For solar modules, cooperation needs to be established with suppliers to decrease the absorption of encapsulation material in short wavelengths without deteriorating the reliability of the solar module.

6. Conclusions

In the photovoltaic industry, an antireflection coating consisting of three SiN_x layers with different refractive indexes is generally adopted to reduce the reflectance and raise the efficiency of monocrystalline silicon PERC solar cells. However, because of the physical constraint of SiN_x , a refractive index as low as about 1.40 cannot be achieved, which is the optimal value for the third layer of triple-layer antireflection coating. Therefore, in this report, the third layer is replaced by SiO_x , which possesses a more appropriate refractive index of 1.46, and it can be easily integrated into the SiN_x deposition process with the PECVD method. Through simulation and analysis with SunSolve, three different thicknesses, i.e., 20 nm, 30 nm, and 40 nm, were selected to construct the SiO_x third layer. Compared with 15 nm SiN_x , the SiO_x third layer can increase the short-circuit current of the solar cell, resulting in a higher conversion efficiency. Although the solar cell efficiency increases along with the increasing thickness of the SiO_x third layer, a 30 nm thickness is the optimal choice because it has very similar efficiency gains and consumes less raw materials compared to a 40 nm thickness. The replacement of 15 nm SiN_x with 30 nm SiO_x as the third layer of antireflection coating can bring about an efficiency gain of 0.15%. According to the reflectance and EQE measurements, this efficiency improvement originates from the reflectance reduction and spectral response enhancement below about 550 nm wavelength. However, the IQE declines below about 400 nm on the contrary, which could be ascribed to the parasitic absorption increase induced by SiO_x . As for the solar module, because the EVA encapsulation material absorbs light in short wavelengths, the spectral response advantage of solar cells with 30 nm SiO_x is partially covered up, resulting in a slightly lower CTM ratio and an output power gain of only 0.9 W for the solar module. The LID and PID test results show

that this new kind of triple-layer antireflection coating will not negatively affect the reliability of the solar module, and it can be applied in mass production.

Author Contributions: Investigation and writing—original draft preparation, S.Z., Y.Y., and D.H.; Conceptualization and methodology, W.L. and H.Q.; supervision, J.J.; project administration, Q.W.; resources, Z.N.; writing—review and editing, X.Z. and L.X.

Funding: This work was supported by the National Natural Science Foundation of China (NSFC, 91833303).

Conflicts of Interest: The authors declare no conflict of interest.

References

1. Lien, S.; Wuu, D.; Yeh, W.; Liu, J. Tri-layer Antireflection Coatings ($\text{SiO}_2/\text{SiO}_2-\text{TiO}_2/\text{TiO}_2$) for Silicon Solar Cells Using a Sol-gel Technique. *Sol. Energy Mater. Sol. Cells* **2006**, *90*, 2710–2719. [[CrossRef](#)]
2. Ali, K.; Khan, S.A.; Mat Jafri, M.Z. Enhancement of Silicon Solar Cell Efficiency by Using Back Surface Field in Comparison of Different Antireflective Coatings. *Sol. Energy* **2014**, *101*, 1–7. [[CrossRef](#)]
3. Hocine, D.; Belkaid, M.S.; Pasquinelli, M.; Escoubas, L.; Simon, J.J.; Rivière, G.A.; Moussi, A. Improved Efficiency of Multicrystalline Silicon Solar Cells by TiO_2 Antireflection Coatings Derived by APCVD Process. *Mater. Sci. Semicond. Proc.* **2013**, *16*, 113–117. [[CrossRef](#)]
4. Richards, B.S. Single-material TiO_2 Double-layer Antireflection Coatings. *Sol. Energy Mater. Sol. Cells* **2003**, *79*, 369–390. [[CrossRef](#)]
5. Lee, B.G.; Skarp, J.; Malinen, V.; Li, S.; Choi, S.; Branz, H.M. Excellent Passivation and Low Reflectivity $\text{Al}_2\text{O}_3/\text{TiO}_2$ Bilayer Coatings for n-Wafer Silicon Solar Cells. In Proceedings of the 38th IEEE Photovoltaic Specialists Conference, Austin, TX, USA, 3–8 June 2012.
6. Zhang, G.; Zhao, J.; Green, M.A. Effect of Substrate Heating on the Adhesion and Humidity Resistance of Evaporated MgF_2/ZnS Antireflection Coatings and on the Performance of High-efficiency Silicon Solar Cells. *Sol. Energy Mater. Sol. Cells* **1998**, *51*, 393–400. [[CrossRef](#)]
7. Bouhafs, D.; Moussi, A.; Chikouche, A.; Ruiz, J.M. Design and Simulation of Antireflection Coating Systems for Optoelectronic Devices: Application to Silicon Solar Cells. *Sol. Energy Mater. Sol. Cells* **1998**, *52*, 79–93. [[CrossRef](#)]
8. Kuo, T.-W.; Wang, N.-F.; Tsai, Y.-Z.; Hung, P.-K.; Houng, M.-P. Broadband Triple-layer $\text{SiO}_x/\text{SiO}_x\text{Ny}/\text{SiN}_x$ Antireflective Coatings in Textured Crystalline Silicon Solar Cells. *Mater. Sci. Semicond. Proc.* **2014**, *25*, 211–218. [[CrossRef](#)]
9. Lelièvre, J.F.; Fourmond, E.; Kaminski, A.; Palais, O.; Ballutaud, D.; Lemiti, M. Study of the Composition of Hydrogenated Silicon Nitride $\text{SiN}_x:\text{H}$ for Efficient Surface and Bulk Passivation of Silicon. *Sol. Energy Mater. Sol. Cells* **2009**, *93*, 1281–1289. [[CrossRef](#)]
10. Zhang, D.; Digdaya, I.A.; Santbergen, R.; van Swaaij, R.A.C.M.M.; Bronsveld, P.; Zeman, M.; van Roosmalen, J.A.M.; Weeber, A.W. Design and Fabrication of a SiO_x/ITO Double-layer Anti-reflective Coating for Heterojunction Silicon Solar Cells. *Sol. Energy Mater. Sol. Cells* **2013**, *117*, 132–138. [[CrossRef](#)]
11. SunSolve. Available online: <https://www.pvlighthouse.com.au/sunsolve> (accessed on 6 February 2019).



© 2019 by the authors. Licensee MDPI, Basel, Switzerland. This article is an open access article distributed under the terms and conditions of the Creative Commons Attribution (CC BY) license (<http://creativecommons.org/licenses/by/4.0/>).